Efficient and Accurate Pattern Synthesis of Circular Antenna Array Employing Iterative Fast Segmented Cyclic Convolution

Jialu Sun, Yanhui Liu, *Senior Member, IEEE*, Qianke Luo, Yi Ren, *Senior Member, IEEE*, and Y. Jay Guo, *Fellow, IEEE*

***Abstract*—An iterative fast segmented cyclic convolution (IFSCC) method is presented for accurately and efficiently synthesizing the pattern of a uniformly spaced circular array (USCA) considering directive element patterns as well as mutual coupling. In this method, the transformations between the excitation vector and the USCA pattern are formulated as a fast segmented cyclic convolution (FSCC) and inverse FSCC which can be highly efficiently accomplished by using fast Fourier transform (FFT) and inverse FFT. The IFSCC method overcomes the limitation of FFT in synthesizing USCA patterns without interpolation or approximation processes. Numerical examples of synthesizing different USCA patterns are conducted to validate the effectiveness and efficiency of the proposed method. The synthesis results also demonstrate the advantages of the proposed method.**

***Index Terms*—Circular arrays, conformal antennas, antenna arrays, radiation pattern synthesis.**

I. Introduction

CIRCULAR antenna arrays provide wide-angle or full-angle beam scanning in the azimuth plane, making them highly versatile in high-performance systems [1], [2]. Various advanced techniques have been developed for circular antenna array pattern synthesis, including analytical approaches [3], [4], stochastic optimization algorithms [5]–[11], convex optimization (CO) techniques [12], [13], and alternating projection approach (APA) [14]–[16]. Analytical approaches are computationally efficient but struggle to achieve precise pattern shape control. Stochastic optimization algorithms and CO are flexible for arbitrary antenna arrays but are time-consuming. Additionally, CO cannot be directly applied to shaped mainlobe synthesis. APA is generally faster than stochastic optimization and CO techniques, but it requires numerous repeated computations of array patterns to update the excitation distribution, which constitutes the main time cost of APA.

For applications in complex and changing environments, array pattern shape should be accordingly optimized and updated in a short period of time. As is known, the iterative fast Fourier transform (FFT) method which employs the FFT and inverse FFT to speed up the transformations between excitation distribution and array factor can be considered as the speed-accelerated version of the APA [17]. Combining with the nonuniform FFT (NUFFT) [18] and active element pattern (AEP) expansion method [19], [20], this technique can be extended to unequally spaced array synthesis and even with mutual coupling. However, these extended iterative FFT techniques are currently limited to synthesizing linear and planar arrays. By using NUFFT to synthesize a linear array obtained through the projection of a circular array, and compensating for positional effects of the array elements, circular array synthesis becomes possible [21]. More recently, the NUFFT technique was progressed to speed up the calculation of spherical antenna array factors [22]. Despite the success, the extended NUFFT techniques focus solely on the array factors, and they introduce some approximation errors. To the best of our knowledge, there is a lack of fast algorithms that can apply the FFT to circular array pattern synthesis without any interpolation.

In this work, we present an iterative fast segmented cyclic convolution (IFSCC) method to accurately and efficiently synthesize pattern of the uniformly spaced circular array (USCA) considering directive element patterns and mutual coupling. Fast segmented cyclic convolution (FSCC) and inverse FSCC are introduced to speed up the forward and backward transformations between the excitation vector and the USCA pattern. Although an initial idea for the forward FSCC was described in our brief conference paper [23], this letter presents for the first time detailed derivations of the forward and inverse FSCC as well as the whole pattern synthesis iteration procedure. Numerical examples of synthesizing USCA patterns with different requirements including low sidelobe, shaped mainlobe, and a null are provided to validate the effectiveness and advantages of the proposed method.

II. Formulation and Algorithm

A. Fast Cyclic Convolution for USCA Pattern and Excitation Distribution Computation

Consider a USCA with N elements distributed at a circle of radius R in the xoy plane. Its far-field pattern at xoy plane can be written as

$$AF(\varphi) = \sum_{n=0}^{N-1} w_n a(\varphi - n\Delta\phi) e^{j\beta R\cos(\varphi - n\Delta\phi)} \quad (1)$$

Manuscript received xxx. This work was supported by the National Key Researchand Development Program of China under Grant 2018YFE0207500.

J. Sun and Y. Liu are with the School of Electronic Science and Engineering, University of Electronic Science and Technology of China, Chengdu 611731, China.

Q. Luo was with the Institute of Electromagnetics and Acoustics, Xiamen University, Fujian 361005, China.

Y. Ren is with the School of Electronic Engineering, Xidian University, Xi'an, 710071, China .

Y. Jay Guo is with the Global Big Data Technologies Centre, University of Technology Sydney (UTS), NSW 2007, Australia.

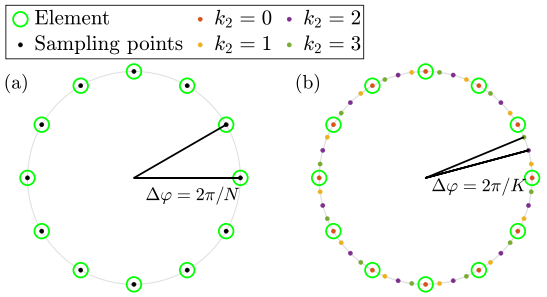

Fig. 1. Schematic diagram of USCA and sampling points. (a) Sampling points φ according to the positions of the USCA elements and (b) Segmented sampling points φ.

where φ is the observation angle away from x-axis, $\Delta\phi = 2\pi/N$ is the uniform angle interval between neighboring elements, $\beta = 2\pi/\lambda$ is the wavenumber in free space, and λ is the wavelength. w_n is the complex excitation for the nth element, and $a(\varphi)$ is the pattern of the first element located at x-axis, which can include mutual coupling when it is obtained by full-wave simulation or measurement in an array environment. In the USCA synthesis, the patterns of different elements can be easily described by rotating $a(\varphi)$ as shown in (1).

Note that (1) does not contain a Vandermonde structure, so it cannot be directly calculated by discrete Fourier transform. To evaluate the array pattern, we uniformly sample φ at an interval of $\varphi = k\Delta\varphi$. If we set $\Delta\varphi = \Delta\phi = 2\pi/N$ as shown in Fig. 1(a), we have $\varphi = 2k\pi/K$ for $k = 0, 1, \cdots, K-1$ where $K = N$. In this case, (1) can be rewritten as

$$AF\left[k\right] = \sum_{n=0}^{N-1} w_n a\left[\left(k-n\right)\frac{2\pi}{N}\right] e^{j\beta R\cos\left[(k-n)\frac{2\pi}{N}\right]}. \quad (2)$$

Thus, by introducing the following two sequences

$$x\left[n\right] = w_n, \quad n = 0, 1, \cdots, N-1 \quad (3)$$

$$h\left[k\right] = a\left[k\cdot\frac{2\pi}{K}\right] e^{j\beta R\cos\left(k\cdot\frac{2\pi}{K}\right)}, \quad k = 0, 1, \cdots, K-1 \quad (4)$$

we can rewrite (2) as the following form

$$\{AF\left[k\right]\} = \{x[k] \circledast h[k]\}_N = \sum_{n=0}^{N-1} x\left[n\right] h\left[k-n\right]. \quad (5)$$

Since the sequence $h[k]$ is periodic with a period of K where $K = N$, if we consider the excitation sequence $x\left[n\right]$ as a periodic function, the summation of (5) can be viewed as the cyclic convolution of two N-length sequences. By applying the cyclic convolution theorem, it can be efficiently computed using FFT and inverse FFT as the following form

$$\{AF\left[k\right]\} = \mathcal{F}^{-1}\left\{\mathcal{F}\left\{x\left[k\right]\right\} \circ \mathcal{F}\left\{h\left[k\right]\right\}\right\} \quad (6)$$

where $\mathcal{F}\{*\}$ and $\mathcal{F}^{-1}\{*\}$ represent FFT and inverse FFT of a sequence, respectively, and the operator "$\circ$" denotes the Hadamard product of two sequences.

The excitation distribution of the array can be easily obtained through the inverse process of (6) as

$$\{x[k]\} = \mathcal{F}^{-1}\left\{\mathcal{F}\{AF[k]\} \oslash \mathcal{F}\{h[k]\}\right\} \quad (7)$$

where the operator "$\oslash$" denotes the Hadamard division of two sequences.

Computation of the array pattern and excitation using the above cyclic convolution can be very efficient. However, in practice, $\Delta\varphi$ should be much smaller than $\Delta\phi$. That is, $K \gg N$. In this situation, the sampled array pattern can be written as

$$AF\left[k\right] = \sum_{n=0}^{N-1} w_n a[2\pi\left(\frac{k}{K} - \frac{n}{N}\right)] e^{j\beta R\cos[2\pi\left(\frac{k}{K}-\frac{n}{N}\right)]}. \quad (8)$$

Note that since $K \neq N$, the above expression is not the form of cyclic convolution anymore, and consequently the FFT-based highly efficient computation technique is not applicable.

B. FSCC and Inverse FSCC for USCA Pattern Synthesis

To overcome the mentioned problem, we develop a segmented fast cyclic convolution (FSCC) and inverse FSCC for efficiently performing the forward and backward transformations between the circular array excitation distribution and pattern. For simplicity, we assume that $K = L \times N$ where L is a positive integer. Here we introduce two auxiliary variables for indexing the pattern sampling points. That is defining $k_1 = \lfloor k/L \rfloor$ and $k_2 = k \mod L$. Then we have $k = k_1 L + k_2$ where $k_1 = 0, 1, \cdots, N-1$ and $k_2 = 0, 1, \cdots, L-1$. By integrating this relation into (5), we obtain

$$AF_{k_2}\left[k_1\right] = \sum_{n=0}^{N-1} w_n a\left[\frac{2\pi((k_1-n)L+k_2)}{NL}\right] \cdot e^{j\beta R\cos\left(\frac{2\pi((k_1-n)L+k_2)}{NL}\right)}. \quad (9)$$

Then, by defining

$$h_{k_2}\left[k_1\right] = a\left[\frac{2\pi\left(k_1 L + k_2\right)}{NL}\right] e^{j\beta R\cos\left(\frac{2\pi(k_1 L+k_2)}{NL}\right)} \quad (10)$$

we have

$$\begin{cases} \{AF_0[k_1]\} = \{x[k_1] \circledast h_0[k_1]\}_N \\ \{AF_1[k_1]\} = \{x[k_1] \circledast h_1[k_1]\}_N \\ \vdots \\ \{AF_{L-1}[k_1]\} = \{x[k_1] \circledast h_{L-1}[k_1]\}_N \end{cases} \quad (11)$$

where $\{AF_{k_2}[k_1]\}$ denotes an N-length decimated pattern sequence whose every element is selected from each L-length segment of the pattern sampling points. The sequences $\{AF_{k_2}[k_1]\}$ with different k_2s constitute the total of NL sampled pattern points. From (11), the sequence $\{AF_{k_2}[k_1]\}$ can be expressed as the N-length cyclic convolution of the excitations $\{x[n]\}$ and the sequence $\{h_{k_2}[k_1]\}$. Thus, for each $k_2 = 0, 1, \cdots, L-1$, we have

$$\{AF_{k_2}[k_1]\} = \mathcal{F}^{-1}\left\{\mathcal{F}\left\{x\left[k_1\right]\right\} \circ \mathcal{F}\left\{h_{k_2}\left[k_1\right]\right\}\right\}. \quad (12)$$

Hence, we can apply the N-point FFT and inverse FFT to speed up the computation of each segment of array pattern samples. This method is called FSCC method.

On the other hand, if the circular array pattern is known, we can also efficiently calculate the excitation sequence by the inverse FSCC as

$$\{x_{k_2}\left[k_1\right]\} = \mathcal{F}^{-1}\{\mathcal{F}\{AF_{k_2}\left[k_1\right]\} \oslash \mathcal{F}\{h_{k_2}\left[k_1\right]\}\}. \quad (13)$$

C. IFSCC Algorithm for USCA Pattern Synthesis

By incorporating the FSCC and inverse FSCC method into the iterative process based on APA [25], we propose an iterative FSCC (IFSCC) method to realize the USCA pattern synthesis. In the qth iteration, firstly, the pattern $AF^{(q-1)}[k]$ of USCA is efficiently obtained by the proposed FSCC method using $w_n^{(q-1)}$. Then $AF^{(q-1)}[k]$ will be revised according to the synthesis requirement such as low sidelobe level (SLL) and so on. For example, we assume the desired amplitudes of the pattern are between the upper bound $\Gamma_U[k]$ and lower bound $\Gamma_L[k]$, then the $AF^{(q-1)}[k]$ can be modified to $AF'[k]$ with the desired boundaries in the following way:

$$AF'[k] = \begin{cases} \xi[k]\Gamma_U[k]\frac{AF^{(q-1)}[k]}{\left|AF^{(q-1)}[k]\right|}, & \text{if } \left|AF^{(q-1)}[k]\right| > \Gamma_U[k] \\ AF^{(q-1)}[k], & \text{if} \Gamma_L[k] \le \left|AF^{(q-1)}[k]\right| \le \Gamma_U[k] \\ \Gamma_L[k]\frac{AF^{(q-1)}[k]}{\left|AF^{(q-1)}[k]\right|} & \text{if } \left|AF^{(q-1)}[k]\right| < \Gamma_L[k] \end{cases} \tag{14}$$

where $\xi[k] \in [0,1]$ is the over modification factor which is used to quickly suppress the SLL. We can impose constraints on the excitation, such as dynamic range ratio (DRR) in the inverse FSCC process. The specific procedure is given in **Algorithm 1**.

In the IFSCC procedure, the $\mathcal{F}\{h_{k_2}[k_1]\}$ calculated in Step 2 does not change with iteration, its computational complexity is not included in the iterative process. If the radix-2 FFT is used, the total number of complex multiplications required for Q iterations is approximately $[0.5Q(N+3K)\log N + 2KQ]$. In comparison, the APA requires $2QNK$ complex multiplications in the same case, where the computational complexity of the projection operator of feasible projection has been ignored because it does not change with iteration. Assume that $L = 15$, the computational complexity of the proposed IFSCC will be lower than that of APA when $N \ge 2$. Although the synthesis procedure may require several hundreds of iterations to achieve the desired pattern performance, this procedure can be implemented very efficiently thanks to the usage of the FSCC. It is important to note that since the IFSCC method is based on the alternating projection framework, it cannot guarantee the global optimality of its synthesized results.

Algorithm 1 Proposed IFSCC for efficient USCA synthesis

1: For a USCA, set the parameters including the oversampling factor L, the total number of samples $K = N*L$, and the desired upper bound $\Gamma_U[k]$ and lower bound $\Gamma_L[k]$ for $k = 0, 1, \cdots, K-1$.
2: Initialize the excitation $w_n^{(0)}$ as the $x^0[n]$, and calculate sequence $h_{k_2}[k_1]$ as (10) for each $k_2 = 0, 1, \cdots, L-1$, where $k_1 = 0, 1, \cdots, N-1$.
3: Set the maximum number of iterations Q, and the current iteration number $q = 1$.
4: Apply the FSCC method in (12) on $x^{(q-1)}[k_1]$ to obtain the $AF_{k_2}^{(q-1)}[k_1]$ for each k_1, k_2, and use $k = k_1 L + k_2$ to obtain the corresponding pattern $AF^{(q-1)}[k]$ of USCA.
5: If the obtained $|AF^{(q-1)}[k]|$ does not exceed the desired bound $\Gamma_L[k]$ and $\Gamma_U[k]$,or $q > Q$, the synthesis procedure will end.
6: Apply the modification method in (14) and obtain $AF'[k]$.
7: Apply the inverse FSCC method in (13) to obtain the corresponding $x'_{k_2}[k_1]$ for each k_1, k_2, and calculate the average excitation sequence as $x'[k_1] = \sum_{k2=0}^{L-1} x'_{k_2}[k_1]/L$.
8: Adjust the $x'[k_1]$ to meet its constraints, such as DRR, or phase-only synthesis, then obtain the final excitation sequence $x^{(q)}[k_1]$ of this iteration.
9: $q = q + 1$, and go back to step 4.

III. Numerical Results

To demonstrate the effectiveness and efficiency of the proposed IFSCC algorithm, we present two examples of synthesizing USCA patterns with varying requirements. In both examples, we set $L = 15$, $Q = 500$, and $\xi = 0.71$.

A. Synthesizing Flat-top Pattern for a 25-element USCA Considering Directional Element Patterns

In the first example, we synthesize a flat-top pattern for a USCA considering directional element patterns. This array has 25 dipole elements uniformly distributed on a 120° arc of a cylinder with radius $R = 18\lambda/\pi$. A flat-top pattern with the mainlobe region of $\mathbf{\Phi_{ML}} = [-25^\circ, 25^\circ]$ was synthesized in [7] by using simulated annealing (SA) method. In [7], the element pattern for the dipole on the cylinder was approximated as

$$a(\varphi) = [1 + 2\max(\cos\varphi, -0.5)]/3. \tag{15}$$

The pattern obtained in [7, Fig. 3] is replotted in Fig. 2(a). Its maximum SLL was -30.0 dB, and the corresponding excitation DRR was 8.35. Then we use the NUFFT to synthesize the same pattern but with an even lower sidelobe level for the same array [21]. We set the same mainlobe region $\mathbf{\Phi_{ML}}$ and set $DRR \le 8.35$. In addition, we consider the desired upper bound of the sidelobe region to be $\Gamma_U^{SL} = -35.0$ dB and the bound of the mainlobe region is $\Gamma_L^{ML} = -1.0$ dB and $\Gamma_U^{ML} = 0$ dB. In the NUFFT method, the number of sampling points is set to 1024. The USCA is converted into a nonuniform linear array, which is then interpolated into a 35-element uniform virtual array. Each real element is approximated by 7 virtual elements. Since the NUFFT only synthesizes array factors, the different element orientations are ignored, leading to errors. Therefore, the obtained SLL for the directional USCA in this example is significantly higher than Γ_U^{SL}, and the mainlobe shape is also unsatisfactory, as shown in Fig. 2(a). The obtained DRR is 8.35. Moreover, the computational time of NUFFT is 0.035 seconds.

Now we apply the proposed IFSCC to synthesize the pattern with the same requirements as used in NUFFT. Here we add 47 virtual elements to the original arc array such that a 72-element USCA occupying the whole circle is generated. The IFSCC is then applied to this fully occupied USCA. We set $K = 1080$ for pattern sampling points. In each iteration, we update the real element excitations and force the virtual element excitations to 0. The pattern obtained using the IFSCC is shown in Fig. 2(a) and the excitation values are stored in the QR code. Compared to the result in [7] and the pattern synthesized by NUFFT, it is obvious that the pattern synthesized by the IFSCC has a much lower SLL while

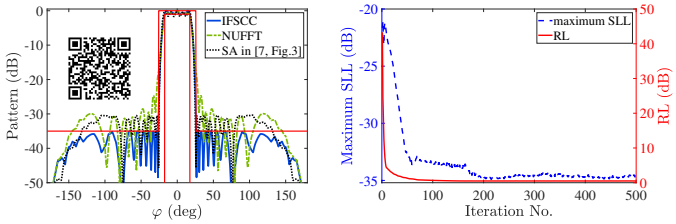

(a) (b)

Fig. 2. (a) The synthesized flat-top patterns by the SA in [7], the NUFFT in [21], and the proposed IFSCC for the 16-dipole-USCA. (b) The curves of achieved pattern performance by the IFSCC. The excitation values of the proposed IFSCC are stored in the quick response (QR) code.

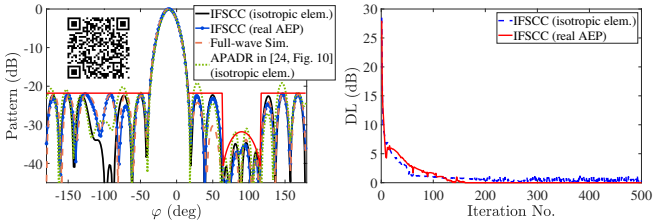

(a) (b)

Fig. 3. (a) The synthesized patterns with shaped-null by the APADR in [24], the IFSCC, and the full-wave simulated pattern using HFSS. (b) The maximum difference between pattern value and upper bound versus the number of iterations. The excitation values of the IFSCC are stored in the QR code.

achieving the desired flat-top beam. To evaluate the beam-shaping accuracy, we define a ripple level (RL) as follow

$$RL = \max_{\varphi \in \mathbf{\Phi}_{ML}} \left| [|AF(\varphi)|]_{dB} - \frac{[\Gamma_L^{ML}]_{dB} + [\Gamma_U^{ML}]_{dB}}{2} \right|. \quad (16)$$

The curves of the maximum SLL and RL for 500 iterations are shown in 2(b). As can be seen, the RL rapidly drops to a very small level, and then the decrease becomes slower since the RL reaches the required value of 0.5 dB. And the SLL has closed to the desired bound at the 215th iteration and more iterations can only provide a very limited improvement. The obtained DRR is 7.20, slightly lower than the preset bound of 8.35. Note that the IFSCC takes 0.040 seconds to accomplish the pattern synthesis in this example, which proves that the IFSCC can achieve more accurate pattern synthesis using a time comparable to that of the NUFFT.

B. Synthesizing Pattern with an Arc-Shaped Null for a 16-element USCA without/with Mutual Coupling

In the second example, we apply the proposed IFSCC to synthesize a pattern with an arc-shaped null for a 16-isotropic-element USCA with a radius of $R = 1.28\lambda$. This pattern was synthesized in [24] by using an auxiliary phase algorithm with DRR reduction (APADR). The obtained pattern in [24, Fig. 10] is re-plotted in Fig. 3. The maximum SLL of the pattern in [24] was -19.1 dB, and the maximum value of its arc-shaped null was -30.9 dB. And the excitation DRR was 4.4. Now, we apply the proposed IFSCC to synthesize the same pattern but with an even lower SLL and deeper notching for the same array. In the proposed method, we adopt the same mainlobe direction of $\varphi_0 = -10^\circ$ and the same mainlobe region of $\mathbf{\Phi_{ML}} = [-36.5^\circ, 16.5^\circ]$ as those in [24]. Then we set $K = 240$. In addition, we set the desired SLL as $\Gamma_U^{SL} = -22.0$ dB, and the maximum value of the null as $\Gamma_U^{Null} = -32.0$ dB. The excitation DRR constraint is kept as $DRR \leq 4.4$. The pattern obtained by the IFSCC is shown in Fig. 3. The maximum SLL is -22.2 dB which is 3.1 dB lower than it in [24], and the peak value of the arc-shaped null is -34.6 dB which is 3.7 dB lower than that it in [24]. The excitation DRR meets the constraint of 4.4. We defined $DL = max\{[|AF(\varphi)|]_{dB} - [\Gamma_U]_{dB}\}$ for $\varphi \notin \mathbf{\Phi_{ML}}$ as the pattern performance index, and the DL versus the number of iterations is shown in Fig. 3(b). As can be seen, the DL reaches a stable state after about 200 iterations. In this example, the IFSCC procedure takes only 0.013 seconds.

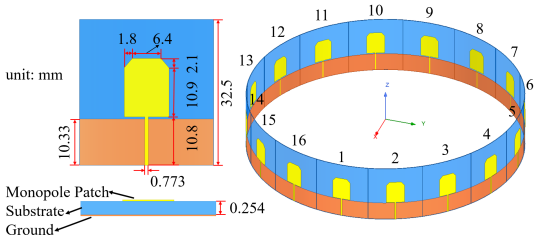

Fig. 4. Geometry of a 16-monopole uniformly spaced circular array.

The proposed IFSCC can also be applicable when considering mutual coupling. To validate this point, we build a USCA with 16 monopole antennas uniformly distributed on a circle of $R = 76.4$ mm, as shown in Fig. 4. The antenna works at 5.0 GHz. The element pattern in the array environment can be extracted by using full-wave simulation. Then, with the same parameters setting, we apply the IFSCC to synthesize the same pattern as above. The obtained pattern for this monopole USCA is also shown in Fig. 3(a) for comparison. It can be seen that the obtained pattern for this monopole array still meets the same preset sidelobe and arc-shaped null bound. The DL versus the number of iterations is also shown in Fig. 3(b). It is obvious that the pattern meets the requirements at the 161th iteration. The synthesis process takes only 0.013 seconds. It can be safely concluded that the proposed IFSCC is still effective for a USCA including mutual coupling.

IV. Conclusion

We have proposed an IFSCC method to accurately and efficiently synthesize USCA patterns. The transformations between excitation vector and USCA pattern are formulated for the first time as FSCC and inverse FSCC, which can be speeded up using FFT and inverse FFT without introducing any approximation errors. Some useful constraints can be easily incorporated into the iterative process of this method. Two examples of synthesizing patterns considering directional elements and even element structure have been conducted to demonstrate the superior accuracy and efficiency of the IFSCC compared to existing algorithms. The proposed method gives an idea to employ the rotationally invariant property of USCA to enable the utilization of FFT in pattern synthesis. This idea could be extended to applications related to circular arrays.

REFERENCES

[1] A. Chepala, Y. Ding, and V. F. Fusco, "Multimode circular antenna array for spatially encoded data transmission," *IEEE Trans. Antennas Propag.*, vol. 67, no. 6, pp. 3863-3868, Jun. 2019.

[2] T. Li, F.-S. Zhang, F. Zhang, Y.-L. Yao, and L. Jiang, "Wideband and high-gain uniform circular array with calibration element for smart antenna application," *IEEE Antennas Wireless Propag. Lett.*, vol. 15, pp. 230-233, 2016.

[3] T. B. Vu, "Side-lobe control in circular ring array," *IEEE Trans. Antennas Propag.*, vol. 41, no. 8, pp. 1143-1145, Aug. 1993.

[4] A. H. Hussein, L. Alnaggar, and M. M. Abd-Elnaby, "Synthesis of circular antenna arrays for realization of broadside Chebyshev linear array patterns in the elevation plane," in *Proc. 37th Nat. Radio Sci. Conf. (NRSC)*, Cairo, Egypt, Sep. 2020, pp. 30-40.

[5] M. Li, Y. Liu, S.-L. Chen, J. Hu, and Y. J. Guo, "Synthesizing shaped-beam cylindrical conformal array considering mutual coupling using refined rotation/phase optimization," *IEEE Trans. Antennas Propag.*, vol. 70, no. 11, pp. 10543-10553, Nov. 2022.

[6] V. V. S. S. S. Chakravarthy and P. M. Rao, "Amplitude-only null positioning in circular arrays using genetic algorithm," in *Proc. IEEE Int. Conf. Electr. Comput. Commun. Technol. (ICECCT)*, Coimbatore, India, Mar. 2015, pp. 1-5.

[7] F. Ares, S. R. Rengarajan, J. A. F. Lence, A. Trastoy, and E. Moreno, "Synthesis of antenna patterns of circular arc arrays," *Electron. Lett.*, vol. 32, no. 20, pp. 1845-1846, Sep. 1996.

[8] G. G. Roy, S. Das, P. Chakraborty, and P. N. Suganthan, "Design of non-uniform circular antenna arrays using a modified invasive weed optimization algorithm," *IEEE Trans. Antennas Propag.*, vol. 59, no. 1, pp. 110-118, Jan. 2011.

[9] T. Zheng *et al.*, "IWORMLF: Improved invasive weed optimization with random mutation and levy flight for beam pattern optimizations of linear and circular antenna arrays," *IEEE Access*, vol. 8, pp. 19460-19478, Jan. 2020.

[10] Z. Liang, J. Ouyang, and F. Yang, "A hybrid GA-PSO optimization algorithm for conformal antenna array pattern synthesis," *J. Electromagn. Waves Appl.*, vol. 32, no. 13, pp. 1601-1615, Apr. 2018.

[11] Y.-Y. Bai, S. Xiao, C. Liu, and B.-Z. Wang, "A hybrid IWO/PSO algorithm for pattern synthesis of conformal phased arrays," *IEEE Trans. Antennas Propag.*, vol. 61, no. 4, pp. 2328-2332, Apr. 2013.

[12] Y. Liu *et al.*, "Synthesis of multibeam sparse circular-arc antenna arrays employing refined extended alternating convex optimization," *IEEE Trans. Antennas Propag.*, vol. 69, no. 1, pp. 566-571, Jan. 2021.

[13] X. Zhao, Q. Yang, and Y. Zhang, "Design of non-uniform circular antenna arrays by convex optimization," in *Proc. 10th Eur. Conf. Antennas Propag. (EuCAP)*, Davos, Switzerland, Apr. 2016, pp. 1-4.

[14] R. Vescovo, "Reconfigurability and beam scanning with phase-only control for antenna arrays," *IEEE Trans. Antennas Propag.*, vol. 56, no. 6, pp. 1555-1565, Jun. 2008.

[15] G. Buttazzoni and R. Vescovo, "Power synthesis for reconfigurable arrays by phase-only control with simultaneous dynamic range ratio and near-field reduction," *IEEE Trans. Antennas Propag.*, vol. 60, no. 2, pp. 1161-1165, Feb. 2012.

[16] G. Buttazzoni and R. Vescovo, "An efficient and versatile technique for the synthesis of 3D copolar and crosspolar patterns of phase-only reconfigurable conformal arrays with DRR and near-field control," *IEEE Trans. Antennas Propag.*, vol. 62, no. 4, pp. 1640-1651, Apr. 2014.

[17] W. P. M. N. Keizer, "Fast low-sidelobe synthesis for large planar array antennas utilizing successive fast Fourier transforms of the array factor," *IEEE Trans. Antennas Propag.*, vol. 55, no. 3, pp. 715-722, Mar. 2007.

[18] K. Yang, Z. Zhao, and Q. H. Liu, "Fast pencil beam pattern synthesis of large unequally spaced antenna arrays," *IEEE Trans. Antennas Propag.*, vol. 61, no. 2, pp. 627-634, Feb. 2013.

[19] X. Huang, Y. Liu, P. You, M. Zhang, and Q. H. Liu, "Fast linear array synthesis including coupling effects utilizing iterative FFT via least-squares active element pattern expansion," *IEEE Antennas Wireless Propag. Lett.*, vol. 16, pp. 804-807, 2017.

[20] J. Bai, Y. Liu, Y. Ren, Z. Nie, and Y. J. Guo, "Efficient synthesis of linearly polarized shaped patterns using iterative FFT via vectorial least-square active element pattern expansion," *IEEE Trans. Antennas Propag.*, vol. 69, no. 9, pp. 6040-6045, Sep. 2021.

[21] S.-R. Wu, C.-C. Huang, J. Mar, and J.-H. Chou, "A versatile pattern synthesis algorithm for circular antenna array," *Int. J. RF Microw. Comput. Aid. Eng.*, vol. 28, e21254, 2018.

[22] F. Yang, S. Yang, W. Long, Y. Chen, S. Qu, and J. Hu, "A novel 3-D-NUFFT method for the efficient calculation of the array factor of conformal arrays," *IEEE Trans. Antennas Propag.*, vol. 69, no. 10, pp. 7047-7052, Oct. 2021.

[23] Q. Luo, Y. Liu, F. Liu, Y. Ren, and Y. J. Guo, "Fast synthesis algorithm for uniformly spaced circular array with low sidelobe pattern," in *Proc. Int. Appl. Comput. Electromagn. Soc. Symp.-China (ACES)*, Beijing, China, 2018, pp. 1-2.

[24] M. Comisso and R. Vescovo, "Fast iterative method of power synthesis for antenna arrays," *IEEE Trans. Antennas Propag.*, vol. 57, no. 7, pp. 1952-1962, Jul. 2009.

[25] O. M. Bucci, G. Franceschetti, G. Mazzarella, and G. Panariello, "Intersection approach to array pattern synthesis," *Proc. Inst. Elect. Eng.*, vol. 137, no. 6, pt. H, pp. 349-357, Dec. 1990.